Dynamics, Analytical Solutions and Choice of Parameters for Towed Space Debris with Flexible Appendages

Vladimir S. Aslanov*, Vadim V. Yudintsev*

34, Moskovskoye shosse, Samara, 443086, Russia

Abstract

Active debris removal is one of the promising techniques that will decrease the population of large, non-functional spacecraft (space debris) on orbit. Properties of space debris should be taken into account during planning an active debris removal mission. In this paper the thrusting phase of tethered deorbit of large space debris with flexible appendages is considered. The goal of the work is to investigate the mutual influence of the tether vibrations and the vibrations of flexible appendages during thrusting phase. A mathematical model of the space tug and the towed space debris with flexible appendages is developed. Parameters of the system are determined with assumptions that the system is moving in straight line, avoiding high amplitude vibrations of flexible appendages. The expression of the discriminant indicates that the vibrations of the tether and flexible appendages influence each other. A critical tether stiffness exists for the given space tug mass that should be avoided.

Keywords: Space debris, Tether, Space tug, Flexible appendages, Vibrations

Note 1

*Corresponding author

Email addresses: aslanov_vs@mail.ru (Vladimir S. Aslanov), yudintsev@classmech.ru (Vadim V. Yudintsev)

URL: http://aslanov.ssau.ru (Vladimir S. Aslanov)

1. Introduction and problem formulation

There are more than 15,000 large objects in orbit around the Earth. Only 5% of these are active spacecraft, 17% are nonfunctional spacecraft, 13% are orbital stages of rockets and the remaining percentage includes fragments [1]. All these objects are tracked, therefore an active spacecraft or a space station can avoid collision with such objects. The collisions of large space debris with other debris can significantly increase the number of small debris on the Earth orbit. The Fengyun 1C anti-satellite test [2] and the Cosmos-Iridium collision [3] created over 5,000 small objects [4]. The debris cascade effect described by Kessler has begun to occur [5]. Several orbits can be dangerous for new missions therefore large debris should be removed. The removal of five or more large debris per year can reduce the debris population.

The choice of the active debris removal technique depends on properties of space debris. Recently several active debris removal methods have been developed [6–9]. The active debris removal using a space tug with a tether is one of promising techniques to decrease the population of large non-functional satellites on the Earth orbit [10], [1]. The tethered tugging dynamics is considered in [11–13].

Reference [1] noted that there are two types of large space debris: spacecraft and orbital stages. Orbital stages may be more easily deorbited because they don't have large appendages such as antennas and solar panels. The removal of passive spacecraft with flexible appendages is more complex task. The vibrations of the flexible appendages should be considered that may leads to the destruction of the spacecraft and the emergence of an even greater number of small fragments.

The goal of the work is to investigate the influence of the tether vibration and the vibrations of flexible appendages during the thruster-burn phase of active debris removal. We consider the simplest thruster-burn phase when only a constant thrust force acts on the space tug. All other forces and torques (e.g. gravitational) are not taken into account.

Flexible spacecraft problems have received considerable attention. Dynamics of flexible structures considered in [14–17]. In this contribution we use a classical approach to describe the motion of flexible appendages using normal-mode coordinates [18].

The paper is divided on three main parts. In the section 2 the mathematical model of large space debris towed by a space tug is considered. In the section 3 simplified mathematical model is obtained that allows to choose the tether stiffness for the given properties of the space debris to avoid high vibrations of the flexible appendages. In the section 4 several numerical examples are provided.

This paper continues the study began in [19–21]. In [19, 20] were considered an attitude motion of large space debris as a finite sized rigid body during thruster-burn phase. In [21] a mathematical model is developed to perform the preliminary research on the influence of the flexible appendages of space debris to the initial phase of deorbit process.

2. Mathematical model

The studied mechanical system includes a space tug, considered as a particle, a massless elastic tether and a passive spacecraft (space debris), as a rigid body with two flexible appendages (panels). We suppose that the attitude motion of the space tug is controlled by the attitude control system of the tug, so the space tug is considered as a particle. We consider only planar motion of the mechanical system relative to its center of mass under the influence of only a thruster.

Lagrange dynamics are used to derive the angular equations of motion. Fig. 1 illustrates the geometry of the mechanical system relative to an orbital frame Ox_0y_0 which is assumed to be fixed for a short period in comparison with the orbital period of the system.

2.1. The kinetic energy and the potential energy

The kinetic energy of the system is composed of the kinetic energy of the rigid bodies T_b and the kinetic energy of the flexible appendages T_a

$$T = T_a + T_b \tag{1}$$

The kinetic energy of the space tug and space debris are written as

$$T_b = \frac{1}{2}\left(m_1\mathbf{V}_1^2 + m_2\mathbf{V}_2^2 + J\dot{\theta}^2\right) \tag{2}$$

where m_1 and m_2 are masses of the tug and debris, J is the moment of inertia of the debris, θ is the pitch attitude. The velocities of the space tug $\mathbf{V}_1$ and space debris $\mathbf{V}_2$ in the frame Ox_0y_0 are

$$\mathbf{V}_2 = \begin{bmatrix}\dot{x}\\ \dot{y}\end{bmatrix},\ \mathbf{V}_1 = \frac{d\mathbf{r}_1}{dt} \tag{3}$$

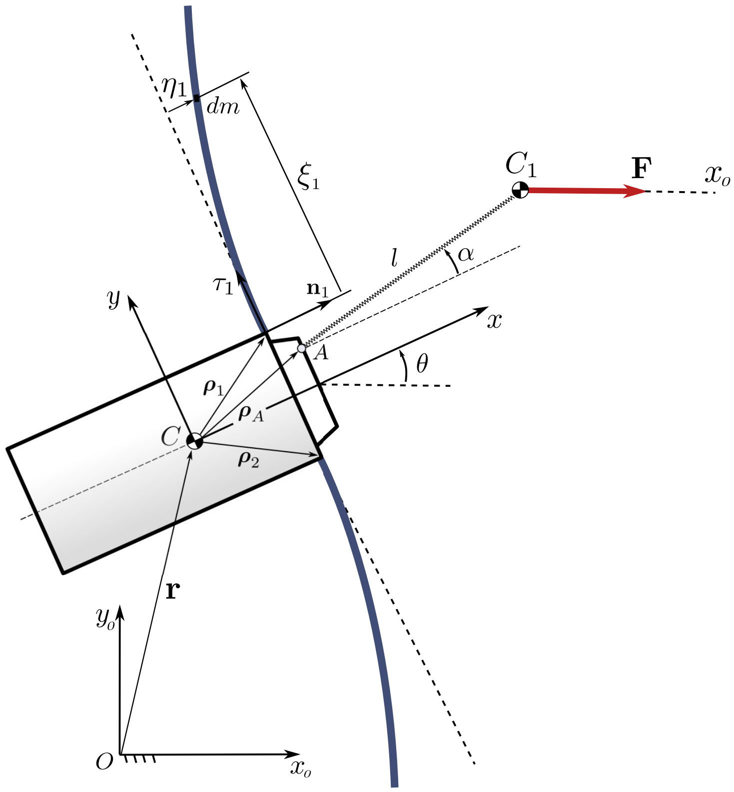

Figure 1: Model of the space debris with flexible appendages

where

$$\mathbf{r}_1 = \mathbf{r}_2 + \mathbf{A}_\theta(\boldsymbol{\rho}_A + \boldsymbol{\tau} l)$$

or

$$\begin{bmatrix} x_1 \\ y_1 \end{bmatrix} = \begin{bmatrix} x \\ y \end{bmatrix} + \begin{bmatrix} \cos\theta & -\sin\theta \\ \sin\theta & \cos\theta \end{bmatrix} \cdot \left(\begin{bmatrix} x_A \\ y_A \end{bmatrix} + l \begin{bmatrix} \cos\alpha \\ \sin\alpha \end{bmatrix} \right) \tag{4}$$

The kinetic energy of the flexible appendages is

$$T_a = \frac{1}{2} \int_0^{l_a} \left(V_{a1}^2 + V_{a2}^2\right) dm \tag{5}$$

where l_a is the length of the flexible appendage (panel), $\mathbf{V}_{ai}$ is the velocity of a differential mass element dm of the flexible appendage i. According to Fig. 1, velocity of an element dm is

$$\mathbf{V}_{ai} = \mathbf{V}_2 + \boldsymbol{\omega} \times (\boldsymbol{\rho}_i + \boldsymbol{\tau}_i \xi_i + \mathbf{n}_i \eta_i) + \mathbf{n}_i \dot{\eta}_i \tag{6}$$

where $\boldsymbol{\rho}_1 = [a, b, 0]^T$, $\boldsymbol{\rho}_2 = [a, -b, 0]^T$ are the vectors of the panel attachment points, $\boldsymbol{\omega} = [0, 0, \dot{\theta}]^T$ is the angular velocity of the space debris.

The potential energy of the considered system consists of two terms: the potential energy of the elastic tether and the potential energy of the flexible appendages

$$U = U_l + U_a \tag{7}$$

The potential energy of the elastic tether is given as

$$U_l = \frac{c_t}{2}(l - l_0)^2 = \frac{1}{2} c_t l_0^2 \varepsilon^2 \tag{8}$$

where c_t is the tether stiffness, $\varepsilon = (l - l_0)/l_0$ is the tether elongation.

The potential energy of the flexible appendages that are considered as beams can be written as

$$U_a = \int_0^{l_a} \left[\sum_{i=1}^{2} E_i J_i \left(\frac{\partial^2 \eta}{\partial \xi^2} \right)^2 \right] d\xi \tag{9}$$

where E_i is an elastic modulus (Young's modulus), J_i is the second moment of area of the beam's cross-section. The deflection of the flexible appendage i is defined as

$$\eta_i = \sum_{j=1}^{N} \Phi_j(\xi_i)\, q_{ij}(t), \quad i = 1, 2 \tag{10}$$

where $q_{ij}(t)$ are modal coordinates, N is the number of the assumed modes considered, and $\Phi_j(\xi_i)$ are shape functions. The following shape function is an acceptable candidate for a clamped-free beam [22, Table 9.4]

$$\Phi_j(\xi_i) = C_j \left[\cosh \frac{\omega_j^{1/2} \xi_i}{l_i} - \cos \frac{\omega_j^{1/2} \xi_i}{l_i} - d_j \left(\sinh \frac{\omega_j^{1/2} \xi_i}{l_i} - \sinh \frac{\omega_j^{1/2} \xi_i}{l_i} \right) \right] \tag{11}$$

where C_j is an unessential constant multiplier that is taken so that $\Phi_j(l_a) = 1$,

$$d_j = \frac{\cos \omega_j^{1/2} + \cosh \omega_j^{1/2}}{\sin \omega_j^{1/2} + \sinh \omega_j^{1/2}}$$

where ω_j is a non-dimensional natural frequency. For the clamped-free beam ω_j defined by the equation [22]

$$\cos \omega_j^{1/2} \cosh \omega_j^{1/2} = -1 \qquad (12)$$

where $\omega_1 = 3.51$, $\omega_2 = 22.03$, $\omega_3 = 61.70, \ldots$ are the roots of the equation (12).

2.2. Lagrange equations and non-potential generalized forces

We use the Lagrangian formalism to write the motion equations of the system

$$\frac{d}{dt}\frac{\partial L}{\partial \dot{s}_i} - \frac{\partial L}{\partial s_i} = Q_i, \quad i = 1, \ldots, 5 + 2N. \qquad (13)$$

where $s = (x, y, \varepsilon, \alpha, \theta, q_{1j}, q_{2j})$ is a generalized coordinates vector, $L = T - U$ is the Lagrangian of the system $\boxed{\text{Note 3}}$

$$\begin{aligned}
L = {} & \frac{1}{3}\mu l_a \left[3(a^2+b^2) + 3bl_a + l_a^2\right] \dot{\theta}^2 + \frac{m_1}{2}\left\{ \frac{J}{m_1}\dot{\theta}^2 + \frac{m_2}{m_1}V_2^2 + \right. \\
& \left[\dot{x} - \dot{\theta}\left(x_a \sin\theta + y_a \cos\theta\right) + l_0\left(\dot{\epsilon}\cos(\alpha+\theta) - (\epsilon+1)\left(\dot{\alpha}+\dot{\theta}\right)\sin(\alpha+\theta)\right)\right]^2 + \\
& \left.\left[\dot{y} + \dot{\theta}\left(x_a \cos\theta - y_a \sin\theta\right) + l_0\left(\dot{\epsilon}\sin(\alpha+\theta) + (\epsilon+1)\left(\dot{\alpha}+\dot{\theta}\right)\cos(\alpha+\theta)\right)\right]^2 \right\} + \\
& \mu l_a V_2^2 + I_1 \mu l_a \left(\dot{x}\cos\theta + \dot{y}\sin\theta\right)\left(\dot{q}_1 + \dot{q}_2\right) + \frac{1}{2} I_2 \mu l_a^2 (\dot{q}_1^2 + \dot{q}_2^2) + \\
& \frac{1}{2}\mu l_a \left\{\dot{y}\left[2a\cos\theta - \sin\theta\left(l_a + 2b\right)\right] - \dot{x}\left[\cos\theta\left(l_a+2b\right) + 2a\sin\theta\right]\right\}\dot{\theta} + \\
& \mu l_a \left(I_1 b + I_3\right)(\dot{q}_2 - \dot{q}_1)\dot{\theta} - U
\end{aligned} \qquad (14)$$

where $q_1 = q_{11}, q_2 = q_{21}$, μ is the linear mass of the beam,

$$\begin{aligned}
I_1 &= \int_0^{l_a} \Phi_1(\xi) d\xi, \quad I_2 = \int_0^{l_a} \Phi_1^2(\xi) d\xi \\
I_3 &= \int_0^{l_a} \xi \Phi_1(\xi) d\xi, \quad I_4 = \int_0^{l_a} \left[\Phi_1''(\xi)\right]^2 d\xi
\end{aligned} \qquad (15)$$

$$\Phi_1(\xi) = \cosh\frac{\omega^{1/2}\xi}{l_a} - \cos\frac{\omega^{1/2}\xi}{l_a} - d\left(\sinh\frac{\omega^{1/2}\xi}{l_a} - \sinh\frac{\omega^{1/2}\xi}{l_a}\right) \qquad (16)$$

where [22]

$$\omega = 3.51,\ d = 0.81 \tag{17}$$

We consider the case when $N = 1$ and take into account only the thrust force $\mathbf{F}$ as a single external force. The non-potential generalized forces are defined as

$$Q_i = \frac{\partial \mathbf{r}_1}{\partial s_i} \cdot \mathbf{F},\ i = 1, \ldots, 7 \tag{18}$$

or in explicit form

$$\begin{aligned}
Q_1 &= F \\
Q_3 &= Fl_0 \cos(\alpha + \theta) \\
Q_4 &= -Fl_0 (1 + \varepsilon) \sin(\alpha + \theta) \\
Q_5 &= -F [x_a \sin\theta + y_a \cos\theta + l_0 (1 + \varepsilon) \sin(\alpha + \theta)] \\
Q_2 &= Q_6 = Q_7 = 0
\end{aligned}$$

3. A simplified mathematical model of the plane motion

It is obvious that in the process of towing the space debris should not be destroyed and its attached elements (solar panels) should not break away. We first focus on the problem of determining the parameters of the system, in which oscillations of the flexible appendages would be the lowest during towing, and assume that the system is moving in a straight line

$$\alpha = 0,\ \theta = 0,\ y = 0 \tag{19}$$

In the next two sections we simplify obtained mathematical model and analyze the influence of the parameters of the system to the vibrations of the flexible appendages of the space debris.

3.1. Governing equations

Considering the conditions (19), the equations of the straight-line motion for the system are

$$M\ddot{x} = F - m_a I_1 (\ddot{q}_1 + \ddot{q}_2) - l_0 m_1 \ddot{\varepsilon} \tag{20}$$

$$m_1 \ddot{x} + l_0 m_1 \ddot{\varepsilon} = F - c_t l_0 \varepsilon \tag{21}$$

$$m_a I_2 \ddot{q}_1 + \mu I_1 \ddot{x} = -EJ l_a I_4 q_1 \tag{22}$$

$$m_a I_2 \ddot{q}_2 + \mu I_1 \ddot{x} = -EJ l_a I_4 q_2 \tag{23}$$

where $m_a = \mu l_a$ is the panel mass. Taking into account that Eqs. (22) and (23) differ only by the variables q_1 and q_2 we can use new variable

$$q = q_1 = q_2$$

and rewrite (20)-(23) as

$$M\ddot{x} = F - 2m_a I_1 \ddot{q} - l_0 m_1 \ddot{\varepsilon} \tag{24}$$
$$m_1 \ddot{x} + l_0 m_1 \ddot{\varepsilon} = F - c_t l_0 \varepsilon \tag{25}$$
$$m_a I_2 \ddot{q} + \mu I_1 \ddot{x} = -EJ l_a I_4 q \tag{26}$$

Now we substitute $\ddot{x}$ from (24) into Eqs. (25)-(26) and yield two second order linear non-homogeneous differential equations with constant coefficients

$$\begin{aligned} \ddot{q} &= c_{qq} q + c_{q\varepsilon} \varepsilon \\ \ddot{\varepsilon} &= c_{\varepsilon q} q + c_{\varepsilon\varepsilon} \varepsilon + a_\varepsilon \end{aligned} \tag{27}$$

where

$$\begin{aligned} a_\varepsilon &= \frac{F}{l_0 m_1} \\ c_{qq} &= \frac{EJ l_a \left(m_2 + 2m_a\right) \mathrm{I}_4}{\mu \left[2m_a \mathrm{I}_1^2 - \left(m_2 + 2m_a\right) l_a \mathrm{I}_2\right]} \\ c_{q\varepsilon} &= \frac{2c_t l_0 \mathrm{I}_1}{2m_a \mathrm{I}_1^2 - \left(m_2 + 2m_a\right) l_a \mathrm{I}_2} \\ c_{\varepsilon q} &= \frac{EJ l_a m_a \mathrm{I}_1 \mathrm{I}_4}{\mu l_0 \left[2m_a \mathrm{I}_1^2 - \left(m_2 + 2m_a\right) l_a \mathrm{I}_2\right]} \\ c_{\varepsilon\varepsilon} &= \frac{c_t l_a \left(M \mathrm{I}_2 - 2\mu \mathrm{I}_1^2\right)}{m_1 \left[2m_a \mathrm{I}_1^2 - \left(m_2 + 2m_a\right) l_a \mathrm{I}_2\right]} \end{aligned} \tag{28}$$

Related homogeneous equations for (27) are written as

$$\begin{aligned} \ddot{q} &= c_{qq} q + c_{q\varepsilon} \varepsilon \\ \ddot{\varepsilon} &= c_{\varepsilon q} q + c_{\varepsilon\varepsilon} \varepsilon \end{aligned} \tag{29}$$

3.2. Analysis

The solution of the homogeneous equation (29) can be taken from [23]

$$\begin{aligned} q &= A_q e^{\lambda t} \\ \varepsilon &= A_\varepsilon e^{\lambda t} \end{aligned} \tag{30}$$

The characteristic equation for (29) is

$$\begin{vmatrix} c_{qq} - \lambda^2 & c_{q\varepsilon} \\ c_{\varepsilon q} & c_{\varepsilon\varepsilon} - \lambda^2 \end{vmatrix} = 0 \tag{31}$$

The equation (31) has the following roots

$$\lambda^2_{(1,2),(3,4)} = \frac{c_{qq} + c_{\varepsilon\varepsilon}}{2} \pm \sqrt{D} \tag{32}$$

where

$$D = \frac{1}{4}(c_{qq} - c_{\varepsilon\varepsilon})^2 + c_{q\varepsilon}c_{\varepsilon q} \tag{33}$$

To examine the roots (32), define the signs of the coefficients (28) which depend on the physical parameters of the system and the definite integrals (15). The integrals (15) depend on the function (16). To simplify the computation of these integrals expand the function (16) in a power series

$$\Phi_1(\xi) = \frac{\omega\xi^2}{l_a^2} - \frac{d\omega^{3/2}\xi^3}{3l_a^3} + O\left(\xi^6\right) = \tilde{\Phi}_1(\xi) + O\left(\xi^6\right) \tag{34}$$

Fig. 2 shows a comparable results between the function $\tilde{\Phi}_1(\xi)$ with the "exact" function $\Phi_1(\xi)$. The ratio error $\varepsilon = (\Phi(\xi) - \Phi^*(\xi))/\Phi(\xi)$ is only 1.5 %.

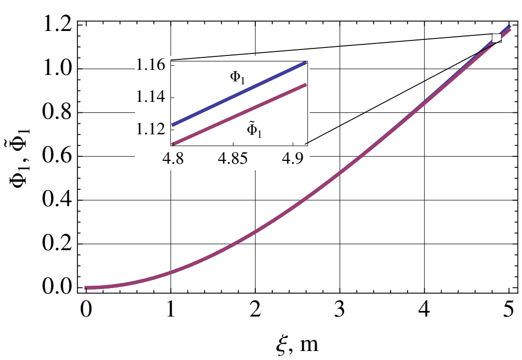

Figure 2: Comparison of the functions $\Phi_1(\xi)$ and $\tilde{\Phi}_1(\xi)$

It is important to note that the sign of the denominator of the coefficients (28) depends on the sign of the function

$$Z(l_a) = 2m_a I_1^2(l_a) - [m_2 + 2m_a]l_a I_2(l_a) \tag{35}$$

Taking into account (15) and (34), the function (35) can be written in the form

$$Z(l_a) = -\left(\frac{1}{5} - \frac{\omega^{1/2}d}{9} + \frac{\omega d^2}{63}\right)\omega^2 m_2 l_a^2 - \\ \left(\frac{8}{45} - \frac{\omega^{1/2}d}{9} + \frac{\omega d^2}{56}\right)\omega^2 \mu l_a^3 + O\left(l_a^4\right) \quad (36)$$

For the mode $N = 1$, and for the values (17), the function (36) may be rewritten in a simple form

$$Z\left(l_a\right) = -0.337 m_2 l_a^2 - 0.267 \mu l_a^3 < 0 \quad (37)$$

Therefore, the denominators of all coefficients (28) are always negative. Similarly, we can find the multiplier $MI_2 - 2\mu I_1^2$, which is included in the numerator of the coefficient c_{ss} from (28)

$$MI_2 - 2\mu I_1^2 = \left(\frac{1}{5} - \frac{\omega^{1/2}d}{9} + \frac{\omega d^2}{63}\right)\left(m_1 + m_2\right)\omega^2 l_a + \\ \left(\frac{8}{45} - \frac{\omega^{1/2}d}{9} + \frac{\omega d^2}{56}\right)\omega^2 \mu l_a^2 + O\left(l_a^4\right)$$

or

$$M\mathrm{I}_2 - 2\mu \mathrm{I}_1^2 = 0.337\left(m_1 + m_2\right) l_a + 0.267 \mu l_a^2 > 0 \quad (38)$$

Thus, according to (37) and (38) all coefficients from (28) are negative

$$c_{qq} < 0,\ c_{q\varepsilon} < 0,\ c_{\varepsilon q} < 0,\ c_{\varepsilon\varepsilon} < 0 \quad (39)$$

The homogeneous equations (29) have periodic solutions, if the roots (32) are less than zero. If the inequalities (39) hold as stated, then one pair of roots (32) is always less than zero, and the other pair is less than zero if

$$|c_{qq} + c_{\varepsilon\varepsilon}| > 2\sqrt{D}$$

or according to (33)

$$c_{qq} c_{\varepsilon\varepsilon} > c_{q\varepsilon} c_{\varepsilon q} \quad (40)$$

After substituting the coefficients (28) into (40) we obtain the following condition

$$\frac{c_t E J M l_a \mathrm{I}_4}{\mu m_1 Z(l_a)} < 0 \quad (41)$$

Taking into account (15) and (37), this condition is always satisfied. Thus, the roots (32) are always less than zero and homogeneous equations (29) have periodic solutions.

After substituting coefficients (28) into (33), the discriminant is written as

$$D = M\frac{4c_t^2\mu^4 I_1^4 + \left[c_t M\mu I_2 - EJm_1\left(M - m_1\right)I_4\right]^2}{4\mu^2 m_1^2\left[\left(M - m_1\right)I_2 - 2\mu \mathrm{I}_1^2\right]^2} + \frac{4c_t\mu^2\mathrm{I}_1^2\left[\mathrm{EJm_1}\left(\mathrm{M} + \mathrm{m_1}\right)\mathrm{I}_4 - \mathrm{c_t M}\mu\mathrm{I}_2\right]}{4\mu^2 m_1^2\left[\left(M - m_1\right)\mathrm{I}_2 - 2\mu\mathrm{I}_1^2\right]^2} \tag{42}$$

The discriminant value (42) indicates the closeness of the roots (32) and hence the degree of influence of the vibrations of the tether and the flexible appendages on each other. A lower value of the discriminant corresponds to closer frequencies (32) that should be avoided. Note 2

3.3. Numerical analysis

We assume that the characteristics of the space debris with the flexible appendages m_2, EJ, l_a, μ are known, then the discriminant (42) can be considered as a function of two variables: the tug mass m_1 and the tether stiffness

$$c_t = \frac{\pi d_T^2 E}{4l_0},$$

where E is a Young's modulus and d_T is the diameter of the tether. Let us consider the tug-tether-debris system with the following parameters presented in Table 1.

The simulation results are depicted in Figs. 3 that shows the discriminant (42) as a function of the tug mass and tether stiffness. The discriminant $D(c_t, m_1)$ has the pronounced minimum. We note that, as follows from (42) the discriminant is a quadratic function of c_t, which reaches the minimum at

$$c_t = -\frac{EJm_1\left[2\mu(2m_1 + m_2 + 2m_a)\mathrm{I}_1^2 - \mathrm{M}(\mathrm{m_2} - 2\mathrm{m_a})\mathrm{I}_2\right]\mathrm{I}_4}{\mu(2\mu\mathrm{I}_1^2 - \mathrm{MI}_2)^2} \tag{43}$$

Fig. 4a shows the discriminant (42) as a function the tether stiffness for the fixed tug mass $m_1 = 450$ kg. A similar dependence of the mass of the tug can be built for the fixed tether stiffness $c_t = 180$ N/m (Fig. 4b).

Taking into account that the expression (42) has been obtained for the simplified case, therefore for the general case of the motion this equation is

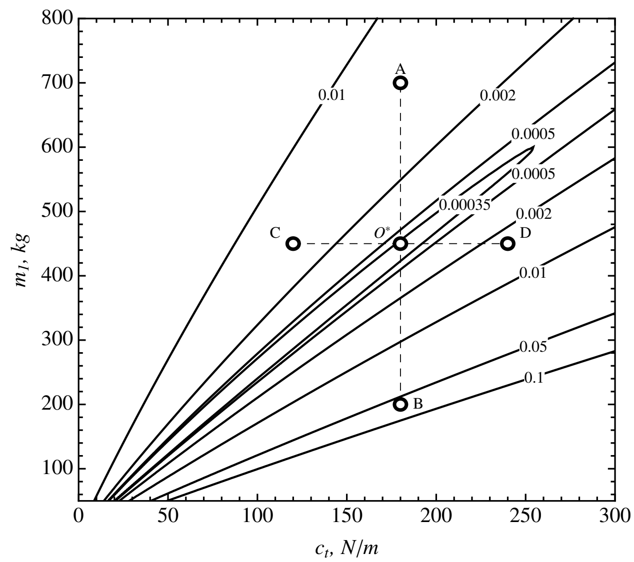

Figure 3: Discriminant $D(c_t, m_1)$ as a function of the tug mass and the tether stiffness

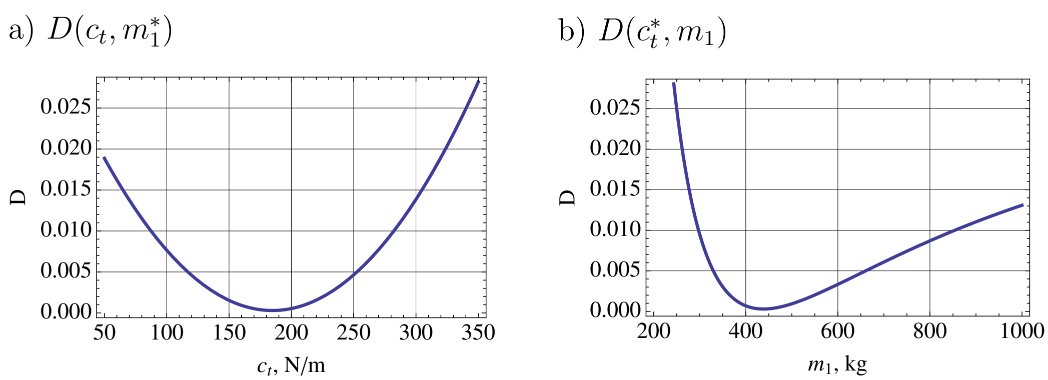

Figure 4: Discriminant $D(c_t, m_1)$ for $c_t = c_t^*$ and $m_1 = m_1^*$

Table 1: Parameters of the space tug and the space debris

Parameter	Value	Parameter	Value
EJ,	184	a, m	1
m_2, kg	2800	b, m	0.1
x_1, m	3	x_2, m	2
y_1, m	0.5	y_2, m	-0.5
l_a, m	5	μ, kg/m	10
x_a, m	2	y_a, m	0
F, N	20	l_0, m	50

an approximate. Obviously, it makes no sense to find a point corresponding to the strictly minimum of the discriminant (42). For future calculations we can take the point O^* in the vicinity of the minimum (Fig. 3)

$$c_t^* = 180\,N/m,\ m_1^* = 450\,kg \tag{44}$$

4. Numerical simulations

To confirm the results of the analysis in the section 3 we perform numerical integration of the motion equations (13) for the following five points in the plane (c_t, m_1) shown in Fig. 3.

Table 2: Parameters of the space tug and the passive spacecraft

Case	Point	c_t	m_1	Figures
1	O^*	c_t^*	m_1^*	5
2	A	c_t^*	$m_1^* + 250\,kg$	6a
3	B	c_t^*	$m_1^* - 250\,kg$	6b
4	C	$c_t^* - 60\,N/m$	m_1^*	6c
5	D	$c_t^* + 60\,N/m$	m_1^*	6d

The initial conditions are

$$q_1 = q_2 = \dot{q}_1 = \dot{q}_2 = 0, \qquad \varepsilon = \dot{\varepsilon} = 0, \qquad \alpha = \dot{\alpha} = 0,$$
$$\theta = 0.1, \qquad \dot{\theta} = 0, \qquad x = \dot{x} = y = \dot{y} = 0$$

The results of the numerical simulation of the planar motion are made for the parameters of the debris, shown in Fig. 5, 6. We note that the

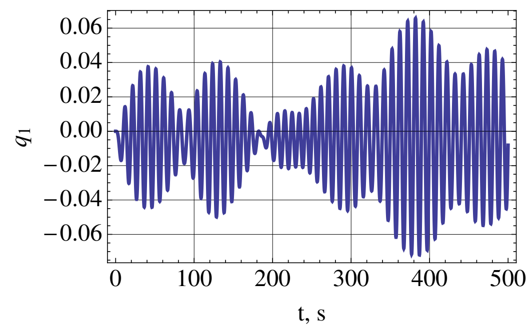

Figure 5: The time history of vibrations of the flexible appendage for Case 1

points A, B, C, D correspond to lower amplitude vibrations of the panel q_1, confirming the analytical predictions using the expression (42). The simulation results confirm the validity of the assumptions on the choice of the tug mass m_1 and tether stiffness c_t. So for the point O^* the flexible appendage vibrate with the largest amplitude in comparison to all the other cases (Fig. 7).

Large vibrations of the flexible appendages lead to damage of the appendage and to the creation of new debris. We note that the thrust tug $\mathbf{F}$ and initial length of the tether l_0 should be selected such that the tether has always been strained.

5. Conclusion

The main contribution of this paper is the formulation of an approach for the study of the motion of a towed satellite with flexible appendages. The mathematical model of the thruster-burn phase is devised that takes into account flexible properties of large space debris. The proposed simplified mathematical model allows to choose the tether stiffness for specific space debris and mass of the space tug. The critical tether stiffness exists for the

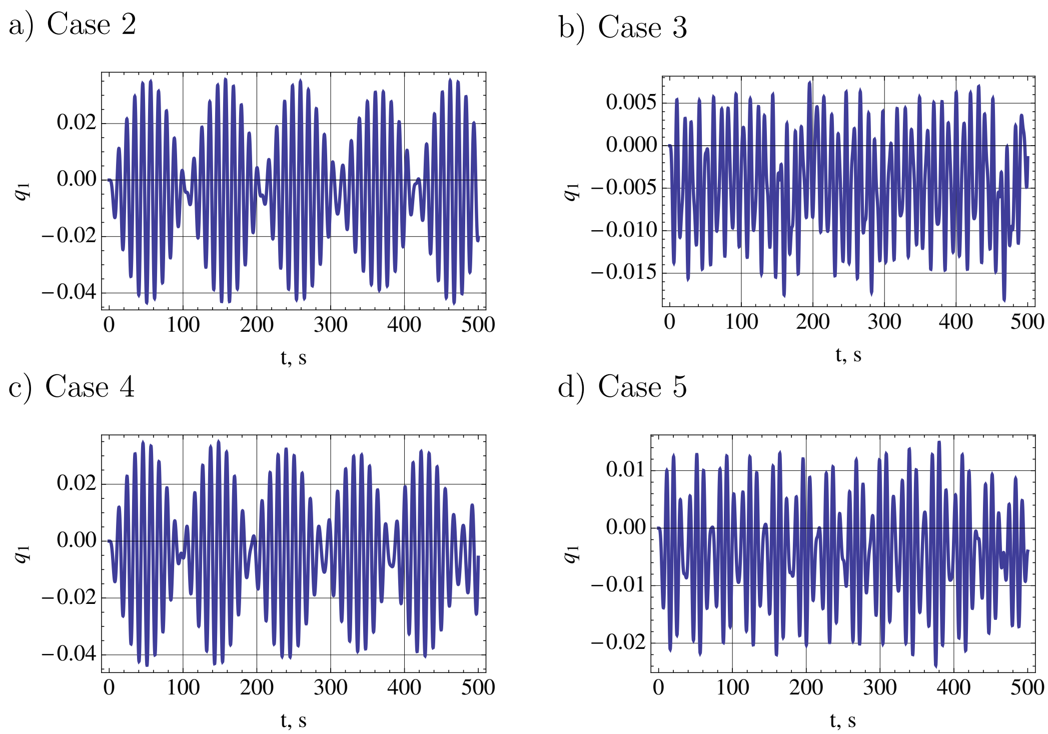

Figure 6: The time history of vibrations of the flexible appendage

given space tug mass which should be avoided. All analytical and numerical results presented in the work were confirmed in good agreement with the direct numerical integration of the original motion equations.

6. Acknowledgements

This work was supported by Ministry of education and science of Russia (Contract no. 9.540.2014/K).

[1] C. Bonnal, J.-M. Ruault, M.-C. Desjean, Active debris removal: Recent progress and current trends, Acta Astronautica 85 (2013) 51–60. doi:10.1016/j.actaastro.2012.11.009.

[2] C. Pardini, L. Anselmo, Evolution of the debris cloud generated by the Fengyun-1C fragmentation event, NASA Space Flight Dynamics Symposium.

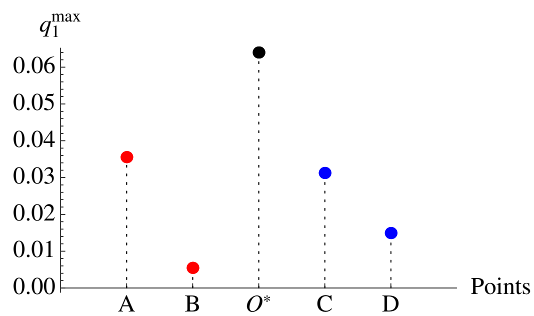

Figure 7: Comparison of the amplitudes of the vibration

[3] N. L. Johnson, Orbital debris: the growing threat to space operations, in: 33rd Annual Guidance and Control Conference, Breckenridge, 2010.

[4] C. Pardini, L. Anselmo, Physical properties and long-term evolution of the debris clouds produced by two catastrophic collisions in Earth orbit, 38th COSPAR Scientific Assembly 38 (2010) 3925.

[5] D. J. Kessler, B. G. Cour-Palais, Collision frequency of artificial satellites: The creation of a debris belt, Journal of Geophysical Research: Space Physics 83 (A6) (1978) 2637–2646. doi:10.1029/JA083iA06p02637.

[6] X. Dafu, K. Xianren, Tether modeling study on electro-dynamic tether deorbiting system, Acta Aeronautica et Astronautica Sinica 5 (2008) 018.

[7] R. L. Forward, R. P. Hoyt, C. W. Uphoff, Terminator Tether : A Spacecraft Deorbit Device, Journal of spacecraft and rockets 37 (2) (2000) 187–196.

[8] L. Iess, C. Bruno, C. Ulivieri, U. Ponzi, M. Parisse, G. Laneve, G. Vannaroni, M. Dobrowolny, F. De Venuto, B. Bertotti, Satellite de-orbiting by means of electrodynamic tethers part I: General concepts and requirements, Acta Astronautica 50 (7) (2002) 399–406.

[9] S. Kitamura, Y. Hayakawa, S. Kawamoto, A reorbiter for large GEO debris objects using ion beam irradiation, Acta Astronautica 94 (2) (2014) 725–735. doi:10.1016/j.actaastro.2013.07.037.

[10] G. Gougnet, D. Alary, D. Gerber, J. Utzmann, A. Wagner, The debritor : an "off the shelf" based multimission vehicle for large space debris removal, 63rd International Astronautical Congress (2012) 1–6.

[11] L. Jasper, H. Schaub, C. Seubert, V. Trushlyakov, E. Yutkin, Tethered tug for large low earth orbit debris removal, in: AAS/AIAA Astrodynamics Specialists Conference, Charleston, 2012.

[12] L. Jasper, H. Schaub, Input shaped large thrust maneuver with a tethered debris object, Acta Astronautica 96 (2014) 128–137. doi:10.1016/j.actaastro.2013.11.005.

[13] L. Jasper, H. Schaub, Discretized input shaping for a large thrust tethered debris object, in: AAS/AIAA Space Flight Mechanics Meeting, AAS, Santa Fe, NM, 2014, pp. 1–20.

[14] P. Grote, J. McUNN, R. Gluck, Equations of motion of flexible spacecraft, Journal of Spacecraft and Rockets 8 (6). doi:10.2514/3.59693.

[15] V. J. Modi, Attitude dynamics of satellites with flexible appendages-a brief review, Journal of Spacecraft and Rockets 11 (11) (1974) 743–751.

[16] J. L. Junkins, Y. Kim, Introduction to dynamics and control of flexible structures, American Institute of Aeronautics and Astronautics, 1993. doi:10.2514/4.862076.

[17] A. Miller, G. Gray, A. Mazzoleni, Nonlinear spacecraft dynamics with a flexible appendage, damping, and moving internal submasses, . . . of Guidance, Control, and Dynamics 24 (3) (2001) 605–615. doi:10.2514/2.4752.

[18] W. C. Hurty, M. F. Rubinstein, Dynamics of Structures, Prentice-Hall international series in engineering, Prentice-Hall, 1964.

[19] V. S. Aslanov, V. V. Yudintsev, Dynamics of Large Debris Connected to Space Tug by a Tether, Journal of Guidance, Control, and Dynamics 36 (6) (2013) 1654–1660. doi:10.2514/1.60976.

[20] V. Aslanov, V. Yudintsev, Dynamics of large space debris removal using tethered space tug, Acta Astronautica 91 (2013) 149–156. doi:10.1016/j.actaastro.2013.05.020.

[21] V. S. Aslanov, V. V. Yudintsev, Behaviour of tethered debris with flexible appendages, Acta Astronautica 104 (1) (2014) 91–98. doi:10.1016/j.actaastro.2014.07.028.

[22] G. Kelly, Fundamentals of mechanical vibrations, McGraw-Hill, 2000.

[23] G. Korn, T. Korn, Mathematical handbook for scientists and engineers: definitions, theorems, and formulas for reference and review, Dover Publications, 2000.